

Porosity-dependent asymmetric thermal buckling of inhomogeneous annular nanoplates resting on elastic substrate

Erfan Salari, Alireza Ashoori and Seyed Ali Sadough Vanini*

Mechanical Engineering Department, Amirkabir University of Technology, Tehran, Iran

(Received May 19, 2018, Revised September 17, 2018, Accepted December 22, 2018)

Abstract. This research is aimed at studying the asymmetric thermal buckling of porous functionally graded (FG) annular nanoplates resting on an elastic substrate which are made of two different sets of porous distribution, based on nonlocal elasticity theory. Porosity-dependent properties of inhomogeneous nanoplates are supposed to vary through the thickness direction and are defined via a modified power law function in which the porosities with even and uneven type are approximated. In this model, three types of thermal loading, i.e., uniform temperature rise, linear temperature distribution and heat conduction across the thickness direction are considered. Based on Hamilton's principle and the adjacent equilibrium criterion, the stability equations of nanoporous annular plates on elastic substrate are obtained. Afterwards, an analytical solution procedure is established to achieve the critical buckling temperatures of annular nanoplates with porosities under different loading conditions. Detailed numerical studies are performed to demonstrate the influences of the porosity volume fraction, various thermal loading, material gradation, nonlocal parameter for higher modes, elastic substrate coefficients and geometrical dimensions on the critical buckling temperatures of a nanoporous annular plate. Also, it is discussed that because of present of thermal moment at the boundary conditions, porous nanoplate with simply supported boundary condition doesn't buckle.

Keywords: nanoporous annular nanoplates; asymmetric buckling; thermal loading; analytical solution; nonlocal theory

1. Introduction

Functionally graded materials (FGMs), a new member of advanced composite materials, that possesses microscopical heterogeneity initiated by a group of Japanese scientists. During the past decade, structures made of FGMs have attracted tremendous attention from research and engineering communities due to their unique advantages offered by smooth and continuously graded distribution of material composition along one or more directions (Ebrahimi and Salari 2015a).

The materials that contain pores are defined as porous materials. Porosities occurring inside the structure during fabrication have a significant effect on mechanical performance of inhomogeneous structures. Nowadays, there has been a great research effort to analyze static, buckling and vibration of scale-free FG structures with porosity (Ebrahimi *et al.* 2016). Among them, Wattanasakulpong and Ungbhakorn (2014) applied a differential transform method (DTM) for linear and nonlinear vibration of elastically end restrained FGM beams with porosities based on the modified power law function. They showed that the porosity volume fraction results in lower natural frequencies. Wattanasakulpong and Chaikittiratana (2015) investigated flexural vibration analysis of porous FG beams based on Timoshenko beam theory and using Chebyshev collocation method (CCM), under two types of porosity

distributions and boundary conditions.

As mentioned before, investigation of mechanical behavior of scale-free plates has been extensively conducted in the literature based on conventional continuum theories. However, these theories are impotent to describe the size effects on the nanostructures. Therefore, higher-order continuum mechanics approach was widely used in the modelling of small-scale structures. In general, these theories can be categorized into four different classes namely the strain gradient family, microcontinuum, surface elasticity and nonlocal elasticity theories (Fang and Zhu 2017). In addition, the nonlocal elasticity theory was improved by Eringen (1983). Nonlocal elasticity theory was initially formulated in an integral form and later reformulated by Eringen (1983) in a differential form by considering a specific kernel function. The nonlocal elasticity theory has been broadly applied to examine the mechanical behaviors of nanoscale structures (Ehyaei *et al.* 2016, Bouadi *et al.* 2018, Aydogdu *et al.* 2018, Reddy 2007, Civalek and Demir 2011, Akgoz and Civalek 2016, Fang *et al.* 2018a, Zhu *et al.* 2017). Recently, Mercan and Civalek (2017) developed the harmonic differential quadrature method (HDQ) for the stability of the silicon carbide nanotube based on the Euler-Bernoulli beam model for different boundary conditions in conjunctions with the surface effect and nonlocal elasticity theory. Also, Mercan and Civalek (2016) presented a simple mechanical model for buckling behavior of boron nitride nanotube (BNNT) surrounded by an elastic matrix based on the Euler-Bernoulli beam theory. The separation of variables and method of discrete singular convolution (DSC) were used to

*Corresponding author, Professor,
E-mail: sadough@aut.ac.ir

solve the governing equations for critical buckling loads of boron nitride nanotube.

Moreover, remarkable development in the application of structural components such as FG beams and FG plates in the orders of micron and sub-micron in micro/nano electro-mechanical systems (MEMS/ NEMS), due to their prominent chemical, mechanical, and electrical properties, led to a provocation in modeling of micro/nano scale structures (Lü *et al.* 2009). Consequently, understanding buckling, vibration and bending analysis of such structures is of great importance in the research community.

The governing equations of structures derived from the aforementioned size-dependent models can be solved using either analytical methods or numerical approaches (Civalek 2006, 2008, 2013, 2017, Gürses *et al.* 2009, Baltacioglu *et al.* 2010, 2011, Akgoz and Civalek 2011a). In the category of FGM structures, Kiani and Eslami (2013) employed an analytical approach for thermal buckling analysis of FGM annular plates resting on elastic foundation based on the classical continuum theory. They reported that only fully clamped plates made of FGMs exhibit the bifurcation-type buckling. Also, a unified solution method for the vibration analysis of the FGM circular, annular and sector plates with general boundary conditions was presented by Wang *et al.* (2016) based on first-order shear deformation theory. Effects of material non-homogeneity and two-parameter elastic foundation on the fundamental frequency parameters of the simply supported beams were studied by Avcar (2016) based on Timoshenko beam theory. Discrete singular convolution for buckling analysis was also presented for simply supported conical panels. This model was employed by Demir *et al.* (2016) to study the effect of geometric and material parameters on critical buckling load of isotropic, composite laminated and functionally graded panels. Shahba *et al.* (2011) employed the finite element method to solve the governing equations of the axially functionally graded tapered Euler-Bernoulli beam for free vibration and stability of FG beams with different boundary conditions. The asymmetrical buckling behavior of isotropic homogeneous annular plates resting on a partial Winkler-type elastic foundation under uniform temperature rise was presented by Bagheri *et al.* (2017). In another work, Bagheri *et al.* (2018) studied the buckling analysis of FG annular plates resting on partial Winkler-type elastic foundation under uniform temperature elevation based on first order shear deformation plate theory. Chen and Li (2013) investigated the micro-scale free vibration analysis of composite laminated Timoshenko beam model based on the new modified couple stress theory. Akgoz and Civalek (2011b) developed modified strain gradient elasticity and modified couple stress theories for the buckling analysis of single walled carbon nanotubes. Thermal stability analysis of FG microplate under the action of thermal loading was discussed by Ashoori and Vanini (2016a) based on the modified couple stress theory. In another work, Ashoori and Vanini (2017a) studied the nonlinear bending, postbuckling and snap-through of circular FG piezoelectric microplates on the basis of the modified couple stress theory. Also, Shen *et al.* (2018) proposed a size-dependent model of clamped-clamped composite laminated electro-static Euler-Bernoulli

microbeams with piezoelectric layers based on a new modified couple stress theory and generalized differential quadrature method for anisotropic elasticity.

Latterly, researchers have studied static and dynamic analysis of perfect FG nanostructures based on the nonlocal elasticity theory (Ebrahimi and Salari 2015b, 2016a, Dastjerdi and Akgoz 2018). For instance, thermo-electro-mechanical vibration characteristics of functionally graded piezoelectric Timoshenko nanobeams subjected to in-plane thermal loads and applied electric voltage were studied by Ebrahimi and Salari (2016b). Post-buckling behavior of FG nanobeams with the von-Kármán geometric nonlinearity was illustrated by Li and Hu (2017) based on Euler-Bernoulli beam model. Additionally, the mechanical buckling analysis of circular and annular FG nanoplates under uniform compressive in-plane loads was presented by Bedroud *et al.* (2015). It is observed that the critical buckling loads for FG nanoplates may be axisymmetric or asymmetric. Fang *et al.* (2018b) examined the surface energy effect on the nonlinear buckling and postbuckling behavior of functionally graded piezoelectric cylindrical nanoshells subjected to lateral pressure based on the electro-elastic surface/interface theory together with von-Kármán-Donnell-type kinematics of nonlinearity. Also, Ashoori *et al.* (2016) presented thermal stability analysis of perfect FG annular nanoplates based on the nonlocal theory. It is found that the critical buckling load decreases by increasing the value of the nonlocal parameter. Due to the existence of porosities in FGMs, it is important to consider porosity effect when analyzing the mechanical behavior of porous FGM structures.

While aforementioned researches were conducted assuming a perfect state for the nanomaterials, observations demonstrate that there is porosity inside the material during the fabrication of structures even at nanoscale (Zhang *et al.* 2014). Examination of porosity effect in analysis of micro/nanostructures is a novel topic which is presented by only a few researchers. Among those research papers, application of higher-order rectangular plate theory in free vibration analysis of porous FG nanoplates is examined by Mechab *et al.* (2016). They stated that the influence of porosity parameter on the frequencies is prominent for FG nanostructures. She *et al.* (2018) presented the vibration behaviors of porous nanotubes in thermal environment based on nonlocal strain gradient theory in conjunction with a refined beam model. It was shown that the presence of porosity can increase or decrease the natural frequency, depending upon the value of volume fraction index. Recently, Shojaeefard *et al.* (2017) implemented modified couple stress theory to model the free vibration and thermal buckling response of a porous FG circular microplate. The GDQ method and nonlinear temperature distribution are used to achieve the critical buckling temperatures and frequencies corresponding to different porosity parameters and aspect ratios. This work is limited to symmetrical thermal buckling of microplates and as we demonstrate next, due to the bending-stretching coupling of FG plates, bifurcation buckling does not take place for FG plates with simply supported boundary condition. It can be evaluated from the literature survey that there is no study on the

asymmetric thermal buckling of nanoporous annular nanoplates resting on elastic substrate via nonlocal elasticity theory.

In view of the above, the aim of the present article is to develop a nanoporous annular nanoplate resting on elastic substrate for asymmetric thermal buckling analysis of thin porous nanoplates within the framework of nonlocal elasticity theory. It is supposed that two different sets of porosity distribution, namely, even and uneven distribution, are considered based on modified power law function. Eringen's elasticity theory is served to study the nano-scale effect. Also, three types of thermal loading are taken into account, i.e., uniform temperature rise, linear temperature distribution and heat conduction across the thickness direction. Additionally, the equilibrium equations of annular nanoplates with porosities are derived utilizing Hamilton's principle and von-Kármán geometric nonlinearity. After a pre-buckling study is accomplished, suitable boundary conditions are chosen to assure the existence of bifurcation point. Then the nonlocal porosity-dependent stability equations are derived via the adjacent equilibrium criterion and the resulting equations are solved by using exact analytical solution. A parametrical study is carried out to examine the influence of porosity parameters, nonlocality for higher modes, various thermal loading, material gradation, elastic substrate coefficients and geometrical dimensions on the structural performance of such nanoporous annular systems. The results of this paper can be a good reference for designing and optimizing the elastic NEMSS.

2. Theory and formulation

2.1 Porosity-dependent functionally graded materials

An annular FG nanoplate on Winkler-Pasternak elastic substrate with porosities is under investigation. Inner radius, outer radius, and thickness of the nanoplate are denoted by, respectively, b , a , and h , as shown in Fig. 1. The material at the upper surface ($z = h/2$) is full ceramic (Al_2O_3) and that at the lower surface ($z = -h/2$) is full metal (Al). Polar

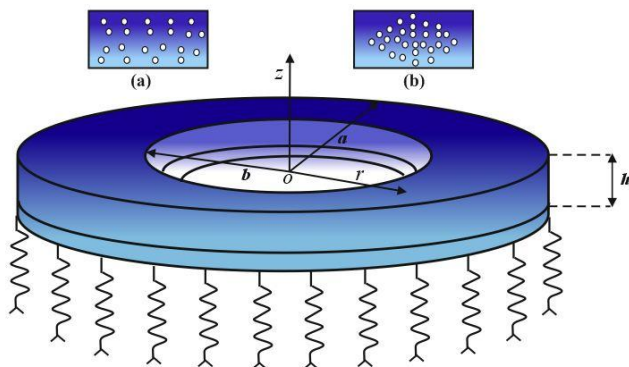


Fig. 1 Configuration of nanoporous annular nanoplate on elastic substrate: (a) Porosity-I; (b) Porosity-II coordinate system (r, θ, z) is applied to the nanoplate where

the origin is located at the mid-surface center of the plate. Also, the annular nanoplate is assumed to contain porosities that disperse evenly (see Fig. 1(a)) or unevenly (see Fig. 1(b)) through the nanoplate thickness direction.

Assuming porosities spread equally among the metal and ceramic phases, the thermo-mechanical effective material properties of the nanoporous annular plate, with a porosity volume fraction α ($\alpha \ll 1$), gives the modified function (Wattanasakulpong and Ungbhakorn 2014)

$$P = P_c \left(V_c - \frac{\alpha}{2} \right) + P_m \left(V_m - \frac{\alpha}{2} \right) \quad (1)$$

where P_c and P_m are the material properties of the ceramic and metal constituents, respectively; and V_c and V_m are volume fractions of ceramic and metal, respectively. Also, the volume fractions of constituents are defined as $V_c + V_m = 1$. The constituent volume fraction of the ceramic and metal phases of annular FG nanoplate is supposed to be expressed as

$$V_c = \left(\frac{z}{h} + \frac{1}{2} \right)^p, \quad V_m = 1 - V_c \quad (2)$$

Using Eqs. (1) and (2), the general material properties of the porous FG nanoplate can be written as

$$P(z) = (P_c - P_m) \left(\frac{z}{h} + \frac{1}{2} \right)^p + P_m - (P_c + P_m) \frac{\alpha}{2} \quad (3)$$

For the annular nanoplate with evenly distributed porosities (Porosity-I), the effective material properties such as Young's modulus E , thermal expansion coefficient α_T and thermal conductivity κ are stated as

$$\begin{aligned} E(z) &= (E_c - E_m) \left(\frac{z}{h} + \frac{1}{2} \right)^p + E_m - \frac{\alpha}{2} (E_c + E_m) \\ \alpha_T(z) &= (\alpha_{Tc} - \alpha_{Tm}) \left(\frac{z}{h} + \frac{1}{2} \right)^p + \alpha_{Tm} - \frac{\alpha}{2} (\alpha_{Tc} + \alpha_{Tm}) \\ \kappa(z) &= (\kappa_c - \kappa_m) \left(\frac{z}{h} + \frac{1}{2} \right)^p + \kappa_m - \frac{\alpha}{2} (\kappa_c + \kappa_m) \end{aligned} \quad (4)$$

where p is the non-negative power law exponent which determines the material variation profile through the thickness of the nanoplate.

In the uneven distribution of porosities (Porosity-II) developed by (Wattanasakulpong and Chaikittiratana 2015), the material properties in Eq. (4) can be replaced by the following forms

$$\begin{aligned} E(z) &= (E_c - E_m) \left(\frac{z}{h} + \frac{1}{2} \right)^p + E_m - \frac{\alpha}{2} (E_c + E_m) \left(1 - \frac{2|z|}{h} \right) \\ \alpha_T(z) &= (\alpha_{Tc} - \alpha_{Tm}) \left(\frac{z}{h} + \frac{1}{2} \right)^p + \alpha_{Tm} - \frac{\alpha}{2} (\alpha_{Tc} + \alpha_{Tm}) \left(1 - \frac{2|z|}{h} \right) \\ \kappa(z) &= (\kappa_c - \kappa_m) \left(\frac{z}{h} + \frac{1}{2} \right)^p + \kappa_m - \frac{\alpha}{2} (\kappa_c + \kappa_m) \left(1 - \frac{2|z|}{h} \right) \end{aligned} \quad (5)$$

From above definition, it can be mentioned that porosity

phases spreading mostly nearby the middle zone of the cross-section and the amount of porosity seems to be linearly decrease to zero at the top and bottom of the cross-section (Wattanasakulpong and Chaikittiratana 2015).

2.2 The nonlocal theory

Considering the stress tensor at a reference point x in the domain of material dependent to strain tensor at all other points in the domain, and considering the interaction between different points of a material, the Eringen's nonlocal elasticity theory was introduced by (Eringen 1983).

These assumptions have made the nonlocal theory one of the most credited theories in studying nanostructures and for that reason, in this paper, the nonlocal elasticity theory is implemented to study the annular nanoplate in which for an elastic solid the nonlocal stress-strain relationship is expressed as

$$\sigma_{ij} = \int_v \alpha(|x' - x|, \tau) t_{ij}(x') dv(x') \quad (6)$$

$\alpha(|x' - x|, \tau)$ is nonlocal kernel function, which contains the small scale effects incorporating into constitutive equations the nonlocal effects at the reference point x produced by local strain at the source x' , and $|x' - x|$ is the Euclidean distance. $\tau = e_0 a / l$ is defined as scale constant, where e_0 is a material constant which is determined experimentally or approximated by matching the dispersion curves of plane waves with those of atomic lattice dynamics; and a and l are the internal and external characteristic length (e.g., lattice spacing and wavelength) of the nanostructures, respectively. σ_{ij} is the nonlocal stress tensor at the reference point and t_{ij} is the classical stress tensor at local point. In addition, the conventional stress tensor is defined in the following way

$$t = C : \varepsilon \quad (7)$$

where C is the fourth order elasticity tensor and $\cdot \cdot$ denotes the double dot product. For the type of physically admissible kernel α , it is possible to express the integral constitutive relation given by Eq. (6) in an equivalent differential form as

$$(1 - \mu \nabla^2) \sigma = C : \varepsilon, \quad \mu = (e_0 a)^2 \quad (8)$$

where $\nabla^2 = \partial^2 / \partial r^2 + 1 / r \partial / \partial r + 1 / r^2 \partial^2 / \partial \theta^2$ is the Laplacian operator in the polar coordinate system and the size effect is taken into consideration using the nonlocal parameter as $\mu = (e_0 a)^2$. Based on the nonlocal theory and plane stress assumption, the nonlocal thermoelastic constitutive equations of porous FG nanoplates subjected to thermal loadings can be represented as (Eringen 1983)

$$\begin{Bmatrix} \sigma_{rr} \\ \sigma_{\theta\theta} \\ \tau_{r\theta} \end{Bmatrix} - \mu \nabla^2 \begin{Bmatrix} \sigma_{rr} \\ \sigma_{\theta\theta} \\ \tau_{r\theta} \end{Bmatrix} = \frac{E(z)}{1 - \nu^2} \begin{bmatrix} 1 & \nu & 0 \\ \nu & 1 & 0 \\ 0 & 0 & (1 - \nu)/2 \end{bmatrix} \begin{Bmatrix} \varepsilon_{rr} \\ \varepsilon_{\theta\theta} \\ \gamma_{r\theta} \end{Bmatrix} - \Theta \begin{Bmatrix} \alpha_T(z) \\ \alpha_T(z) \\ 0 \end{Bmatrix} \quad (9)$$

where $\Theta = T - T_0$ denotes the temperature rise and T and T_0

are the temperature distribution and reference temperature, respectively. Furthermore, the parameter $e_0 a$ is the scale coefficient revealing the small scale effect on the responses of structures of nanosize. The value of the small-scale parameter depends on boundary condition, chirality, mode shapes, number of walls, and the nature of motions. The parameter $e_0 = (\pi^2 - 4)^{1/2} / 2\pi \cong 0.39$ was given by Eringen (1983). The nonlocal parameter, $\mu = (e_0 a)^2$, is experimentally obtained for various materials; for instance, a conservative estimate of $\mu < 4$ (nm)² for a single-walled carbon nanotube is proposed (Wang 2005). There is no rigorous study made on estimating the value of small scale to simulate mechanical behaviour of functionally graded micro/nanoplates (Ebrahimi and Salari 2015b). Hence all researchers who worked on size-dependent mechanical behaviour of FG nanoplates based on the nonlocal elasticity method investigated the effect of small scale parameter on mechanical behaviour of FG nanoplates by changing the value of the small scale parameter. In the present study, a conservative estimate of the small-scale parameter is considered to be in the range of 0–4 (nm)² (Bedroud *et al.* 2015).

2.3 Kinematic assumptions and equilibrium equations

Displacement field in the nanoplate domain is assumed to obey the classical plate theory (CPT). Based on the CPT, the displacement components of the nanoplate may be considered as

$$\begin{aligned} u(r, \theta, z) &= u_0(r, \theta) - z w_{0,r}(r, \theta) \\ v(r, \theta, z) &= v_0(r, \theta) - \frac{z}{r} w_{0,\theta}(r, \theta) \\ w(r, \theta, z) &= w_0(r, \theta) \end{aligned} \quad (10)$$

where (u_0, v_0, w_0) are the displacements along the (r, θ, z) -directions on the mid-surface of the porous nanoplate.

Buckling of structures is a nonlinear phenomenon and thus a geometrically nonlinear formulation must be presented. Also, the von-Kármán geometric nonlinearity, consistent with the small strains, and large displacements in the polar coordinates system, takes the form

$$\begin{aligned} \varepsilon_{rr} &= u_{,r} + \frac{1}{2} w_{,r}^2 \\ \varepsilon_{\theta\theta} &= \frac{1}{r} v_{,\theta} + \frac{1}{r} u + \frac{1}{2r^2} w_{,\theta}^2 \\ \gamma_{r\theta} &= \frac{1}{r} u_{,\theta} + v_{,r} - \frac{1}{r} v + \frac{1}{r} w_{,\theta} w_{,r} \end{aligned} \quad (11)$$

where ε_{rr} and $\varepsilon_{\theta\theta}$ are the radial and circumferential normal strains and $\gamma_{r\theta}$ denotes the shear strain component. In these equations, a comma indicates the partial derivative with respect to its afterwards. For a classical plate theory, the components of stress resultants are related to the stress field through the following equations

$$(N_{rr}, N_{\theta\theta}, N_{r\theta}) = \int_{-h/2}^{h/2} (\sigma_{rr}, \sigma_{\theta\theta}, \tau_{r\theta}) dz \quad (12)$$

$$(M_{rr}, M_{\theta\theta}, M_{r\theta}) = \int_{-h/2}^{h/2} (\sigma_{rr}, \sigma_{\theta\theta}, \tau_{r\theta}) z dz \quad (12)$$

Substitution of Eq. (9) into Eq. (12) with the aid of Eqs. (10) and (11), obtains the nonlocal stress resultants in terms of the mid-plane displacements of the porous annular nanoplate as

$$(1-\mu\nabla^2) \begin{pmatrix} N_{rr} \\ N_{\theta\theta} \\ M_{rr} \\ M_{\theta\theta} \\ M_{r\theta} \end{pmatrix} = \frac{1}{1-\nu^2} \begin{bmatrix} E_0 & \nu E_0 & 0 & E_1 & \nu E_1 & 0 \\ \nu E_0 & E_0 & 0 & \nu E_1 & E_1 & 0 \\ 0 & 0 & \frac{1-\nu}{2} E_0 & 0 & 0 & \frac{1-\nu}{2} E_1 \\ E_1 & \nu E_1 & 0 & E_2 & \nu E_2 & 0 \\ \nu E_1 & E_1 & 0 & \nu E_2 & E_2 & 0 \\ 0 & 0 & \frac{1-\nu}{2} E_1 & 0 & 0 & \frac{1-\nu}{2} E_2 \end{bmatrix} \begin{pmatrix} u_{0,r} + \frac{1}{2} w_{0,r}^2 \\ \frac{1}{r} v_{0,\theta} + \frac{1}{r} u_{0,\theta} + \frac{1}{2r^2} w_{0,\theta}^2 \\ \frac{1}{r} u_{0,\theta} + v_{0,r} - \frac{1}{r} v_{0,\theta} + \frac{1}{r} u_{0,\theta} w_{0,r} \\ -w_{0,r} \\ \frac{1}{r^2} w_{0,\theta\theta} - \frac{1}{r} w_{0,r} \\ \frac{2}{r} w_{0,r\theta} + \frac{2}{r^2} w_{0,\theta} \end{pmatrix} \begin{pmatrix} N^T \\ N^T \\ M^T \\ M^T \\ 0 \end{pmatrix} \quad (13)$$

In the above equation, N^T and M^T are the thermally induced force and moment and E_0 , E_1 and E_2 are constant coefficients, which are given below

$$\begin{aligned} (E_0, E_1, E_2) &= \int_{-h/2}^{h/2} E(z) (1, z, z^2) dz \\ (N^T, M^T) &= \frac{1}{1-\nu} \int_{-h/2}^{h/2} E(z) \alpha_T(z) \Theta(1, z) dz \end{aligned} \quad (14)$$

Static version of Hamilton's principle, also known as the virtual displacement principle, may be employed to obtain the nonlinear equilibrium equations of the nanoplate with porosities. Therefore, for an equilibrium position of porous FG nanoplate on elastic substrate the following identity should be satisfied (Ashoori and Vanini 2016b)

$$\delta \Pi = 0 \quad (15)$$

where Π is the total potential energy and δ shows the variation symbol. Here, the total potential energy can be defined as the summation of two different parts: the strain energy which results from the stresses of porous nanoplate U_s and the strain energy due to the elastic substrate U_F . Consequently, the first variation of this energy may be written according to the following form

$$\begin{aligned} \delta(U_s + U_F) &= \int_b^a \int_0^{2\pi} \int_{-h/2}^{h/2} (\sigma_{rr} \delta \varepsilon_{rr} + \sigma_{\theta\theta} \delta \varepsilon_{\theta\theta} + \tau_{r\theta} \delta \gamma_{r\theta}) r dz d\theta dr \\ &+ \int_b^a \int_0^{2\pi} \left(K_g (w_{0,r} \delta w_{0,r} + \frac{1}{r^2} w_{0,\theta} \delta w_{0,\theta}) + K_w w_0 \delta w_0 \right) r dr d\theta \end{aligned} \quad (16)$$

where K_w and K_g denote the Winkler constant and the Pasternak constant of the surrounding elastic substrate, respectively.

Substituting Eqs. (10)-(12) into Eq. (16) and taking the variation of u_0 , v_0 and w_0 , integrating the resulting expression by parts and setting the coefficients of δu_0 , δv_0 and δw_0 equal to zero, a set of equations for the equilibrium state of the porous annular nanoplate resting on elastic substrate are obtained as follows

$$\begin{aligned} \delta u_0: \quad N_{r,r} + \frac{1}{r} (N_{rr} - N_{\theta\theta}) + \frac{1}{r} N_{r\theta,r} &= 0 \\ \delta v_0: \quad \frac{1}{r} N_{\theta\theta,\theta} + \frac{2}{r} N_{r\theta} + N_{r\theta,r} &= 0 \end{aligned} \quad (17)$$

$$\begin{aligned} \delta w_0: \quad M_{r,r} + \frac{2}{r} M_{r,r} + \frac{1}{r^2} M_{\theta\theta,\theta\theta} - \frac{1}{r} M_{\theta\theta,r} + \frac{2}{r} M_{r\theta,r} \\ + \frac{2}{r^2} M_{r\theta,\theta} + N_{rr} w_{0,r} + N_{\theta\theta} \left(\frac{1}{r^2} w_{0,\theta\theta} + \frac{1}{r} w_{0,r} \right) \\ + 2N_{r\theta} \left(\frac{1}{r} w_{0,r\theta} - \frac{1}{r^2} w_{0,\theta} \right) + K_g \left(w_{0,r} + \frac{1}{r} w_{0,r} + \frac{1}{r^2} w_{0,\theta\theta} \right) - K_w w_0 = 0 \end{aligned} \quad (17)$$

3. Pre-buckling analysis

Pre-buckling deformations and stresses should be obtained to assure the occurrence of primary-secondary equilibrium path. Only the flat pre-buckling configurations are considered in the present paper, which lead to bifurcation-type buckling. In the pre-buckling state of bifurcation-type buckling, if occurs, of initially flat annular nanoplates, the mid-plane must be undeflected, i.e.

$$w_0^0(r, \theta) = 0 \quad (18)$$

here, a superscript 0 is adopted to indicate the primary equilibrium path characteristics. Also, the pre-buckling state must be symmetric due to the symmetry of thermal loading. This implies that

$$v_0^0(r, \theta) = 0 \quad (19)$$

It should be noted that if nanoplates with porosity are to undergo in-plane compressive thermal loads, radial immovability is needed. Therefore, solving Eqs. (13) and (17) for immovable in-plane boundary conditions, provided that the nonlinear terms are set equal to zero, yields

$$u_0^0(r, \theta) = 0 \quad (20)$$

In view of Eq. (13), the nonzero pre-buckling stress resultants are derived as follow

$$\begin{aligned} N_{rr}^0 &= N_{\theta\theta}^0 = -N^T \\ M_{rr}^0 &= M_{\theta\theta}^0 = -M^T \\ N_{r\theta}^0 &= M_{r\theta}^0 = 0 \end{aligned} \quad (21)$$

Generally speaking, the property distribution of the porous nanoplate are graded unsymmetrically with respect to the mid-plane of the plate. Besides, the unsymmetrical distribution of properties results in thermal moments for general types of thermal loading, i.e., uniform temperature rise, linear distribution and heat conduction across the thickness direction. In such conditions, due to bending-stretching coupling of FG nanoplates with porosities, even uniform temperature rise triggers thermal moments defined by Eq. (14). In turn, these thermal moments are responsible for the commencement of deflection prior to the temperature at which buckling phenomenon occurs. In other words, for the case when edge supports are capable of supplying the induced thermal moment prior to stability loss, plate remains undeflected and the bifurcation buckling may occur. According to Eq. (21), only clamped type of out-of-plane boundary conditions supplies the extra

moments when is necessary. Therefore, porous annular nanoplates are assumed to be clamped at both inner and outer edges throughout this research.

4. Adjacent equilibrium criterion and nonlocal stability equations

Adjacent equilibrium criterion is a general tool to obtain the linearized stability equations of the nanoplate associated with the onset of buckling (Brush and Almroth 1975). According to this criterion, each of the displacement components on the primary equilibrium path is perturbed infinitesimally to establish a new equilibrium state. Assume that a pre-buckling equilibrium position of the porous nanoplate is defined in terms of the displacement components u_0^0 , v_0^0 and w_0^0 . Another equilibrium position may exist, adjacent to the primary one. Displacement components of the secondary path differ by u_0^1 , v_0^1 and w_0^1 with respect to the displacement components of the pre-buckling state. As a result, the components of total displacement field are

$$\begin{aligned} u_0 &= u_0^0 + u_0^1 \\ v_0 &= v_0^0 + v_0^1 \\ w_0 &= w_0^0 + w_0^1 \end{aligned} \quad (22)$$

Similar to Eq. (22), the nonlocal stress resultants are divided into the stable equilibrium, and the neighboring state consisting of linear functions of displacements, represented by superscripts 0 and 1, respectively

$$\begin{aligned} N_{rr} &= N_{rr}^0 + N_{rr}^1, & M_{rr} &= M_{rr}^0 + M_{rr}^1 \\ N_{\theta\theta} &= N_{\theta\theta}^0 + N_{\theta\theta}^1, & M_{\theta\theta} &= M_{\theta\theta}^0 + M_{\theta\theta}^1 \\ N_{r\theta} &= N_{r\theta}^0 + N_{r\theta}^1, & M_{r\theta} &= M_{r\theta}^0 + M_{r\theta}^1 \end{aligned} \quad (23)$$

Substituting Eqs. (22) and (23) into equilibrium Eq. (17) and simplifying the results, the stability equations of porous annular plate can be represented as

$$\begin{aligned} N_{r,r}^1 + \frac{1}{r}(N_{rr}^1 - N_{\theta\theta}^1) + \frac{1}{r}N_{r\theta,\theta}^1 &= 0 \\ \frac{1}{r}N_{\theta\theta,\theta}^1 + \frac{2}{r}N_{r\theta}^1 + N_{r\theta,r}^1 &= 0 \\ M_{r,r,r}^1 + \frac{2}{r}M_{r,r}^1 + \frac{1}{r^2}M_{\theta\theta,\theta\theta}^1 - \frac{1}{r}M_{\theta\theta,r}^1 + \frac{2}{r}M_{r\theta,r\theta}^1 & \\ + \frac{2}{r^2}M_{r\theta,\theta}^1 + N_{rr}^0 w_{0,r}^1 + N_{\theta\theta}^0 \left(\frac{1}{r^2}w_{0,\theta\theta}^1 + \frac{1}{r}w_{0,r}^1 \right) & \\ + 2N_{r\theta}^0 \left(\frac{1}{r}w_{0,r\theta}^1 - \frac{1}{r^2}w_{0,\theta}^1 \right) + K_g \left(w_{0,rr}^1 + \frac{1}{r}w_{0,r}^1 + \frac{1}{r^2}w_{0,\theta\theta}^1 \right) - K_w w_0^1 &= 0 \end{aligned} \quad (24)$$

The nonlocal stability equations may be expressed in terms of the displacements. To this end, upon substitution of nonlocal Eq. (13) into Eqs. (24) and eliminating second and higher order terms of incremental displacements, the stability equations of porous annular nanoplates resting on

Winkler-Pasternak elastic substrate are derived as follows

$$\begin{aligned} E_0 \left(\frac{1}{r}u_{0,r}^1 + \frac{1}{r}u_{0,r}^1 - \frac{1}{r^2}u_0^1 - \frac{1}{r^2}v_{0,\theta}^1 + \frac{1}{r}v_{0,r}^1 \right) + \frac{(1-\nu)}{2} E_0 \left(\frac{1}{r^2}u_{0,\theta\theta}^1 - \frac{1}{r}v_{0,r\theta}^1 - \frac{1}{r^2}v_{0,\theta}^1 \right) \\ - E_1 \left(w_{0,rr}^1 - \frac{1}{r^2}w_{0,r}^1 + \frac{1}{r}w_{0,r}^1 - \frac{2}{r^3}w_{0,\theta\theta}^1 + \frac{1}{r^2}w_{0,\theta\theta,r}^1 \right) = 0 \\ E_0 \left(\frac{1}{r^2}v_{0,\theta\theta}^1 + \frac{1}{r}u_{0,r\theta}^1 + \frac{1}{r^2}u_{0,\theta}^1 \right) + \frac{(1-\nu)}{2} E_0 \left(v_{0,rr}^1 + \frac{1}{r}v_{0,r}^1 - \frac{1}{r^2}v_0^1 + \frac{1}{r^2}u_{0,\theta}^1 - \frac{1}{r}u_{0,r\theta}^1 \right) \\ - E_1 \left(\frac{1}{r}w_{0,r\theta}^1 + \frac{1}{r^2}w_{0,r\theta}^1 + \frac{1}{r^3}w_{0,\theta\theta\theta}^1 \right) = 0 \\ \frac{E_1}{1-\nu^2} \left(u_{0,rr}^1 + \frac{2}{r}u_{0,r}^1 - \frac{1}{r^2}u_0^1 - \frac{1}{r^2}u_{0,r}^1 + \frac{1}{r^3}u_{0,\theta\theta}^1 + \frac{1}{r^2}u_{0,\theta\theta,r}^1 - \frac{1}{r^2}v_{0,r\theta}^1 + \frac{1}{r^3}v_{0,\theta}^1 + \frac{1}{r^3}v_{0,\theta\theta\theta}^1 - \frac{1}{r}v_{0,r\theta}^1 \right) \\ - \frac{E_2}{1-\nu^2} \left(w_{0,rr}^1 + \frac{2}{r}w_{0,r}^1 - \frac{1}{r^2}w_{0,r}^1 + \frac{1}{r^3}w_{0,r}^1 + \frac{2}{r^2}w_{0,\theta\theta}^1 - \frac{2}{r^2}w_{0,\theta\theta,r}^1 + \frac{4}{r^4}w_{0,\theta\theta}^1 + \frac{1}{r^4}w_{0,\theta\theta\theta\theta}^1 \right) \\ - N^T \left(w_{0,rr}^1 + \frac{1}{r}w_{0,r}^1 + \frac{1}{r^2}w_{0,\theta\theta}^1 \right) + \mu N^T \nabla^2 \left(w_{0,rr}^1 + \frac{1}{r}w_{0,r}^1 + \frac{1}{r^2}w_{0,\theta\theta}^1 \right) + K_g \left(w_{0,rr}^1 + \frac{1}{r}w_{0,r}^1 + \frac{1}{r^2}w_{0,\theta\theta}^1 \right) \\ - \mu K_g \nabla^2 \left(w_{0,rr}^1 + \frac{1}{r}w_{0,r}^1 + \frac{1}{r^2}w_{0,\theta\theta}^1 \right) - K_w w_0^1 + \mu K_w \left(w_{0,rr}^1 + \frac{1}{r}w_{0,r}^1 + \frac{1}{r^2}w_{0,\theta\theta}^1 \right) = 0 \end{aligned} \quad (25)$$

After mathematical manipulations, three coupled stability equations which are presented in Eq. (25), may be uncoupled to gain one equation in terms of w_0^1 . To achieve a single nonlocal equation, the procedure is presented in the following step by step.

- (1) The first of the stability Eq. (25) is differentiated with respect to r and then divided by r .
- (2) The second of the stability Eq. (25) is differentiated with respect to θ .
- (3) The second of Eq. (25) is divided by r .
- (4) The resulting equations in steps (1)-(3) are added and the result is multiplied by $-E_1 / E_0 (1 - \nu^2)$.
- (5) The derived equation in step (4) is added to the third of nonlocal stability Eq. (25).

The result is the following uncoupled equation in terms of the incremental lateral displacement w_0^1

$$\begin{aligned} D_p \left(w_{0,rrr}^1 + \frac{2}{r}w_{0,rr}^1 - \frac{1}{r^2}w_{0,r}^1 + \frac{1}{r^3}w_{0,r}^1 + \frac{2}{r^2}w_{0,\theta\theta}^1 - \frac{2}{r^2}w_{0,\theta\theta,r}^1 + \frac{4}{r^4}w_{0,\theta\theta}^1 + \frac{1}{r^4}w_{0,\theta\theta\theta\theta}^1 \right) \\ + N^T \left(w_{0,rr}^1 + \frac{1}{r}w_{0,r}^1 + \frac{1}{r^2}w_{0,\theta\theta}^1 \right) - \mu N^T \nabla^2 \left(w_{0,rr}^1 + \frac{1}{r}w_{0,r}^1 + \frac{1}{r^2}w_{0,\theta\theta}^1 \right) - K_g \left(w_{0,rr}^1 + \frac{1}{r}w_{0,r}^1 + \frac{1}{r^2}w_{0,\theta\theta}^1 \right) \\ + \mu K_g \nabla^2 \left(w_{0,rr}^1 + \frac{1}{r}w_{0,r}^1 + \frac{1}{r^2}w_{0,\theta\theta}^1 \right) + K_w w_0^1 - \mu K_w \left(w_{0,rr}^1 + \frac{1}{r}w_{0,r}^1 + \frac{1}{r^2}w_{0,\theta\theta}^1 \right) = 0 \end{aligned} \quad (26)$$

where $D_p = \frac{E_2 - E_1^2 / E_0}{1 - \nu^2}$ is the equivalent flexural rigidity of porous FG nanoplates. For the sake of generality, it is more appropriate to represent the stability equation in a dimensionless form. The following non-dimensional quantities are defined and utilized in the rest of this work

$$\begin{aligned} \rho = \frac{r}{a}, \quad \delta = \frac{h}{a}, \quad \beta = \frac{b}{a}, \quad \eta = \frac{\mu}{a^2}, \quad d = \frac{D_p}{D_0} \\ k_w = \frac{K_w a^4}{D_0}, \quad k_g = \frac{K_g a^2}{D_0}, \quad n^T = \frac{N^T a^2}{D_0} \end{aligned} \quad (27)$$

Considering the newly introduced dimensionless quantities (27), the non-dimensional form of stability Eq. (26) alters to

$$\left[\left(\frac{\partial^2}{\partial \rho^2} + \frac{1}{\rho} \frac{\partial}{\partial \rho} + \frac{1}{\rho^2} \frac{\partial^2}{\partial \theta^2} \right) \left(\frac{\partial^2}{\partial \rho^2} + \frac{1}{\rho} \frac{\partial}{\partial \rho} + \frac{1}{\rho^2} \frac{\partial^2}{\partial \theta^2} + \frac{n^T - k_g - \eta k_w}{d - \eta(n^T - k_g)} \right) + \frac{k_w}{d - \eta(n^T - k_g)} \right] w_0^1(\rho, \theta) = 0 \quad (28)$$

5. Analytical solution methodology

Due to the periodical conditions of the displacement field and considering the fact that the buckling pattern of porous annular nanoplates may be asymmetric (Wang *et al.* 2004), the solution of the displacement field components is considered in the form

$$w_0^1(a\rho, \theta) = W_n(\rho) \cos(n\theta) \quad (29)$$

where n is an integer number which shows the number of nodal diameters. The value of $n = 0$ refers to the symmetric buckled configuration and $n > 0$ indicates the asymmetric buckled shapes of the porous nanoplate. Substituting Eq. (29) into Eq. (28) yields to the following ordinary differential equation in terms of W_n

$$\left(\frac{d^2}{d\rho^2} + \frac{1}{\rho} \frac{d}{d\rho} - \frac{n^2}{\rho^2} + \lambda_1^2 \right) \left(\frac{d^2}{d\rho^2} + \frac{1}{\rho} \frac{d}{d\rho} - \frac{n^2}{\rho^2} + \lambda_2^2 \right) W_n(\rho) = 0 \quad (30)$$

in which its solution depends upon λ_1 and λ_2 . First, the following parameters are defined as

$$B_1 = \frac{n^T - k_g - \eta k_w}{d - \eta(n^T - k_g)}, \quad B_2 = \frac{k_w}{d - \eta(n^T - k_g)} \quad (31)$$

Now, the solution procedures are classified as follows

Solution 1: $k_w = 0, n = 0$

$$W_n(\rho) = c_1 J_0(\lambda\rho) + c_2 Y_0(\lambda\rho) + c_3 \ln \rho + c_4 \quad (32)$$

Solution 2: $k_w = 0, n > 0$

$$W_n(\rho) = c_{1n} J_n(\lambda\rho) + c_{2n} Y_n(\lambda\rho) + c_{3n} \rho^n + c_{4n} \rho^{-n} \quad (33)$$

where

$$\lambda = \sqrt{B_1} \quad (34)$$

and J_n and Y_n are the Bessel functions of the first and second kind, respectively.

Solution 3: $k_w \neq 0, B_1 < 2\sqrt{B_2}$

$$W_n(\rho) = c_{1n} \left(\frac{J_n(\lambda_1\rho) + J_n(\lambda_2\rho)}{2} \right) + c_{2n} \left(\frac{Y_n(\lambda_1\rho) + Y_n(\lambda_2\rho)}{2} \right) \quad (35)$$

$$+ c_{3n} \left(\frac{J_n(\lambda_1\rho) - J_n(\lambda_2\rho)}{2i} \right) + c_{4n} \left(\frac{Y_n(\lambda_1\rho) - Y_n(\lambda_2\rho)}{2i} \right) \quad (35)$$

where

$$\lambda_{1,2} = \sqrt{\frac{B_1 \pm i\sqrt{4B_2 - B_1^2}}{2}} \quad (36)$$

in which $i = \sqrt{-1}$.

Solution 4: $k_w \neq 0, B_1 = 2\sqrt{B_2}$

$$W_n(\rho) = c_{1n} J_n(\lambda\rho) + c_{2n} Y_n(\lambda\rho) + c_{3n} \rho J_{n+1}(\lambda\rho) + c_{4n} \rho Y_{n+1}(\lambda\rho) \quad (37)$$

where

$$\lambda = \sqrt{\frac{B_1}{2}} \quad (38)$$

Solution 5: $k_w \neq 0, B_1 > 2\sqrt{B_2}$

$$W_n(\rho) = c_{1n} J_n(\lambda_1\rho) + c_{2n} Y_n(\lambda_1\rho) + c_{3n} J_n(\lambda_2\rho) + c_{4n} Y_n(\lambda_2\rho) \quad (39)$$

where

$$\lambda_{1,2} = \sqrt{\frac{B_1 \pm \sqrt{B_1^2 - 4B_2}}{2}} \quad (40)$$

Now, from a mathematical point of view, adequate boundary conditions are needed to achieve the stability criterion. As demonstrated previously, it should be pointed out that the porous FG nanoplates commence to deflect at the onset of transverse thermal loading for all types of boundary conditions unless clamped type. In the case of clamped porous annular plate, lateral deflection is zero at both inner and outer edges which can be written as the following mathematical representations

$$W_n(\beta) = \frac{dW_n}{d\rho}(\beta) = W_n(1) = \frac{dW_n}{d\rho}(1) = 0 \quad (41)$$

Applying the above boundary conditions to Eqs. (32), (33), (35), (37) and (39) results in a system of equations in terms of constants c_{in} ($i = 1, 2, 3, 4$). In order to obtain a non-trivial solution, the determinant of the coefficients matrix must be set equal to zero. This nonlinear determinantal equation includes both n^T and n . For every integer number n , the obtained transcendental equation should be solved and its smallest positive root represents critical buckling loads n_{cr}^T .

6. Types of thermal loading

At this stage, three types of temperature profile are obtained for a porous FG nanoplate subjected to thermal boundary condition on its upper and lower surfaces. Each type of thermal loads is presented in the following subsections

6.1 Uniform temperature rise (UTR)

It is assumed that the porous nanoplate being initially at the reference temperature experiences a uniform temperature rise Θ . The temperature change is (Ashoori *et al.* 2017)

$$\Theta(z) = \Theta_{cr} \quad (42)$$

It should be pointed out that even in this type of thermal loading, initiation of thermal loading triggers thermal moments due to the bending-stretching coupling of the porous FG nanoplate.

6.2 Linear temperature distribution (LTD)

It is assumed that the temperature profile varies only

through the thickness, which is compatible with the design requirements of the FGM structures. When the nanoplate with porosity is thin enough, the temperature distribution may be estimated to be linear. Therefore, if T_c and T_m show the temperature of ceramic-rich and metal-rich surfaces respectively, the temperature rise field is specified as follows through the thickness

$$\Theta(z) = T_m - T_0 + \Theta_{cr} \left(\frac{1}{2} + \frac{z}{h} \right) \quad (43)$$

where $\Theta_{cr} = T_c - T_m$.

6.3 Heat conduction (HC) across the thickness

Through-the-thickness heat conduction equation with the known temperature boundary conditions on upper and lower surfaces of the nanoplate in the absence of heat generation takes the form (Ashoori and Vanini 2017b)

$$\frac{d}{dz} \left(\kappa(z) \frac{dT}{dz} \right) = 0 \quad (44)$$

$$T \left(-\frac{h}{2} \right) = T_m, \quad T \left(\frac{h}{2} \right) = T_m + \Theta_{cr} = T_c$$

Employing the power series technique, the solution of this equation is obtained as

$$\Theta(z) = \Theta_{cr} \left[\sum_{i=0}^{\infty} \frac{(-1)^i}{pi+1} \left(\frac{\kappa_c - \kappa_m}{\kappa_m} \right)^i \right]^{-1} \sum_{i=0}^{\infty} \left[\frac{(-1)^i}{pi+1} \left(\frac{1}{2} + \frac{z}{h} \right)^{pi+1} \left(\frac{\kappa_c - \kappa_m}{\kappa_m} \right)^i \right] \quad (45)$$

To assure the convergence of the temperature profile of Eq. (45), sufficient terms of series expansion must be taken into account.

7. Numerical investigation

In this section, we perform the accuracy of the proposed model before proceeding with a detailed parametric investigation. Thus, several numerical examples for the asymmetric thermal buckling of porous annular nanoplates resting on an elastic substrate are carried out, accordingly.

The computed results are then discussed in details. Moreover, the material properties of each constituent in the present paper, including the Young's modulus, Poisson's ratio, thermal expansion coefficient, and thermal conductivity, as listed in Table 1. To assess the effects of size dependency on the thermal buckling behavior of an annular nanoplate, a FGM nanoplate made of Alumina

Table 1 Material properties of nanoplate

Properties	Alumina (Al ₂ O ₃)	Aluminum (Al)
E (GPa)	380	70
α_T (K ⁻¹)	7.4e-6	23.0e-6
κ (Wm ⁻¹ K ⁻¹)	10.4	204
ν	0.3	0.3

(Al₂O₃) and Aluminum (Al) materials is considered. Top surface of the plate is Al₂O₃ rich, while the bottom one is Al rich. The thickness of the porous annular nanoplate is assumed to be 0.5 nm and in the LTD and HC types of thermal loading, the metal surface temperature is raised by 5 K. Also, in the present study, the dimensional foundation parameters for $\delta = 0.015$ are considered to be in the range of 0–7.3357e-13 N/(nm)³ for K_w and 0–7.9886e-11 N/nm for K_g . However, five dimensionless foundation conditions are considered in this examination

$(k_w, k_g) = (0,0)$ (unconstrained), $(k_w, k_g) = (100,0)$ (Winkler), $(k_w, k_g) = (100,10)$ (Pasternak), $(k_w, k_g) = (200,10)$ (Pasternak), $(k_w, k_g) = (200,20)$ (Pasternak)

7.1 Comparison of results

To show the validity and accuracy of the presented method, in Table 2, the critical buckling temperatures of perfect FG annular plates under UTR loading is compared with those reported in Kiani and Eslami (2013) based on the classical continuum theory in which the nonlocal parameter is taken to be zero. For two different magnitudes of power index, i.e., $p = 1, 2$, and different β ratios critical buckling temperatures of a perfect plate are evaluated. As visible from Table 2, the buckling temperatures are in excellent agreement which guarantees the accuracy and correctness of the presented formulation and solution method.

7.2 Parametric studies

After validating the present model for the case of perfect FGM plates, numerical and illustrative examples are given to explore the asymmetric thermal buckling behavior of annular nanoplates with porosities resting on elastic foundation.

Tables 3-4 respectively present the critical buckling temperature difference of in-contact porous annular FG nanoplates under UTR and HC loading corresponding to different values of the nonlocal parameter, various power indexes, β ratio and porosity-I parameter. Nanoplate is resting on the elastic substrate with stiffness $k_w = 100$, $k_g = 10$ and thickness to radius of nanoplate is set equal to $\delta = 0.015$. It is inferred that the fundamental buckled shape of the nanoplate is not associated with a symmetrical shape since in all cases the number of nodal diameters is larger than zero. Also, it is indicated that increasing of nonlocal parameter leads to lower critical buckling temperature

Table 2 Comparison of critical buckling temperature difference of perfect FGM plate under UTR loading ($\delta = 0.015$, $k_w = 100$, $k_g = 10$)

p		β	
		0.3	0.5
1	Present study	90.77776	154.23236
	(Kiani and Eslami 2013)	90.778	154.232
2	Present study	86.26107	141.83852
	(Kiani and Eslami 2013)	86.261	141.839

Table 3 Critical buckling temperature difference Θ_{cr} of nanoporous annular nanoplates under UTR loading for various β ratios, power indices, porosity and nonlocal parameters ($k_w = 100, k_g = 10, \delta = 0.015$). Number of nodal diameters are displayed as superscript

μ (nm) ²	β	α (Porosity-I) = 0.1				α (Porosity-I) = 0.2			
		Power index				Power index			
		1	2	5	10	1	2	5	10
0	0.2	86.3422 ²	83.0358 ²	95.1391 ²	107.0360 ²	101.9708 ²	97.2152 ²	117.9200 ²	146.1562 ²
	0.3	103.6705 ²	97.0923 ³	108.9660 ³	121.4939 ³	120.6876 ³	110.3785 ³	129.3095 ³	158.7784 ³
	0.4	128.6995 ³	118.0427 ³	130.5006 ³	144.5300 ³	147.9909 ³	131.3356 ³	149.7521 ³	182.4854 ³
	0.5	172.7537 ⁴	155.0137 ⁴	168.3846 ⁴	184.9919 ⁴	196.2477 ⁴	168.1478 ⁴	185.3817 ⁴	223.6904 ⁴
2	0.2	80.9052 ²	78.3241 ²	90.1693 ²	101.6512 ²	95.9111 ²	92.3185 ²	112.7009 ³	139.4081 ³
	0.3	94.4344 ³	89.0540 ³	100.5745 ³	112.4478 ³	110.2943 ³	102.1509 ³	120.9791 ³	148.9935 ³
	0.4	112.6786 ³	104.3393 ³	116.2132 ³	129.1378 ³	130.2610 ³	117.3358 ³	135.6200 ³	165.9028 ³
	0.5	141.6543 ⁴	128.5165 ⁴	140.8547 ⁴	155.3847 ⁴	161.9033 ⁴	141.2175 ⁴	158.4208 ⁴	192.1431 ⁴
4	0.2	76.3841 ²	74.4060 ²	86.0362 ²	97.1728 ²	90.8722 ²	88.2460 ²	107.9969 ³	133.8846 ³
	0.3	87.0740 ³	82.7493 ³	93.9926 ³	105.3525 ³	102.1425 ³	95.6976 ³	114.4448 ³	141.3181 ³
	0.4	100.9605 ³	94.3163 ³	105.7629 ³	117.8794 ³	117.2930 ³	107.0960 ³	125.2831 ³	153.7733 ³
	0.5	121.3532 ⁴	111.2196 ⁴	122.8838 ⁴	136.0577 ⁴	139.4838 ⁴	123.6378 ⁴	140.8212 ⁴	171.5495 ⁴

Table 4 Critical buckling temperature difference Θ_{cr} of nanoporous annular nanoplates under HC loading for various β ratios, power indices, porosity and nonlocal parameters ($k_w = 100, k_g = 10, \delta = 0.015$). Number of nodal diameters are displayed as superscript

μ (nm) ²	β	α (Porosity-I) = 0.1				α (Porosity-I) = 0.2			
		Power index				Power index			
		1	2	5	10	1	2	5	10
0	0.2	270.0879 ²	222.5497 ²	208.0891 ²	214.2955 ²	320.0702 ²	251.7142 ²	239.3100 ²	269.9050 ²
	0.3	327.6247 ²	262.6374 ³	240.0089 ³	244.6599 ³	381.8486 ³	287.6452 ³	263.4475 ³	294.0399 ³
	0.4	410.7306 ³	322.3859 ³	289.7223 ³	293.0402 ³	471.9681 ³	344.8505 ³	306.7713 ³	339.3701 ³
	0.5	557.0078 ⁴	427.8231 ⁴	377.1785 ⁴	378.0182 ⁴	631.2487 ⁴	445.3346 ⁴	382.2805 ⁴	418.1582 ⁴
2	0.2	252.0348 ²	209.1125 ²	196.6160 ²	202.9864 ²	300.0692 ²	238.3479 ²	228.2491 ³	257.0019 ³
	0.3	296.9573 ³	239.7132 ³	220.6368 ³	225.6614 ³	347.5435 ³	265.1869 ³	245.7930 ³	275.3303 ³
	0.4	357.5350 ³	283.3052 ³	256.7392 ³	260.7136 ³	413.4474 ³	306.6362 ³	276.8213 ³	307.6624 ³
	0.5	453.7458 ⁴	352.2559 ⁴	313.6251 ⁴	315.8373 ⁴	517.8885 ⁴	371.8245 ⁴	325.1428 ⁴	357.8366 ⁴
4	0.2	237.0232 ²	197.9386 ²	187.0747 ²	193.5810 ²	283.4374 ²	227.2316 ²	218.2800 ³	246.4404 ³
	0.3	272.5178 ³	221.7328 ³	205.4424 ³	210.7599 ³	320.6368 ³	247.5717 ³	231.9450 ³	260.6541 ³
	0.4	318.6265 ³	254.7206 ³	232.6145 ³	237.0689 ³	370.6439 ³	278.6852 ³	254.9145 ³	284.4697 ³
	0.5	386.3382 ⁴	302.9269 ⁴	272.1385 ⁴	275.2467 ⁴	443.8890 ⁴	323.8384 ⁴	287.8442 ⁴	318.4595 ⁴

difference since the nonlocal parameter decreases the stiffness of porous annular nanoplates, especially for annular nanoplates with higher modes of buckled shape and β ratio. In other words, by increasing the influence of small scale effect, the stiffness of annular FG nanoplates decreases. In addition, one can see that the number of nodal diameters becomes larger as the β ratio of the annular nanoplate increases. Also, an increase in the porosity parameter leads to the increase of the critical buckling temperature. This is due to the increase of the porosity which then increases the stiffness of the nanoplate.

In Table 5, the effects of the nonlocal parameter, elastic foundation coefficients and porosity parameter on the critical buckling temperature of FG annular nanoplates subjected to different types of thermal loading are demonstrated. The model parameters $p = 1$ and $\delta = 0.015$ are assumed. As seen for all types of thermal loading, higher modes of buckling configuration occur, i.e., $n > 0$. As expected with increasing the nonlocal parameter of the nanoplate, critical buckling temperature of the plate decreases. It is also observed that the critical buckling temperature of nanoplate from maximum to minimum may be sorted, in order, HC, LTD, and UTR. With increasing

Table 5 Effect of nonlocal parameter and elastic foundation on the critical buckling temperature Θ_{cr} of the Porosity-I annular nanoplate subjected to different types of thermal loading and porosity parameters ($\beta = 0.3, p = 1, \delta = 0.015$). Number of nodal diameters are displayed as superscript

μ (nm) ²	Load type	$\alpha = 0$			$\alpha = 0.1$			$\alpha = 0.2$		
		(k_w, k_s)			(k_w, k_s)			(k_w, k_s)		
		(0,0)	(100,10)	(200,20)	(0,0)	(100,10)	(200,20)	(0,0)	(100,10)	(200,20)
0	UTR	67.5450 ²	90.7777 ²	113.0682 ³	74.0624 ²	103.6705 ²	131.7908 ³	81.6409 ²	120.6876 ³	157.7617 ³
	LTD	117.3010 ²	160.8733 ²	202.6783 ³	128.3491 ²	183.3742 ²	235.6343 ³	140.6584 ²	212.3206 ³	280.3623 ³
	HC	208.7083 ²	286.2343 ²	360.6161 ³	229.3143 ²	327.6247 ²	420.9950 ³	252.9675 ²	381.8486 ³	504.2183 ³
2	UTR	59.5492 ²	82.4691 ²	104.3661 ³	65.2951 ²	94.4344 ³	122.1878 ³	71.9764 ²	110.2943 ³	147.0782 ³
	LTD	102.3052 ²	145.2908 ²	186.3577 ³	112.0555 ²	166.2094 ³	217.7877 ³	122.9213 ²	193.2458 ³	260.7550 ³
	HC	182.0268 ²	258.5092 ²	331.5776 ³	200.2034 ²	296.9573 ³	389.1094 ³	221.0682 ²	347.5435 ³	468.9555 ³
4	UTR	53.2460 ²	75.8972 ³	97.5406 ³	58.3838 ²	87.0740 ³	114.6557 ³	64.3579 ²	102.1425 ³	138.6984 ³
	LTD	90.4839 ²	132.9654 ³	173.5568 ³	99.2111 ²	152.5304 ³	203.7896 ³	108.9391 ²	178.2848 ³	245.3755 ³
	HC	160.9937 ²	236.5792 ³	308.8015 ³	177.2551 ²	272.5178 ³	364.0997 ³	195.9219 ²	320.6368 ³	441.2963 ³

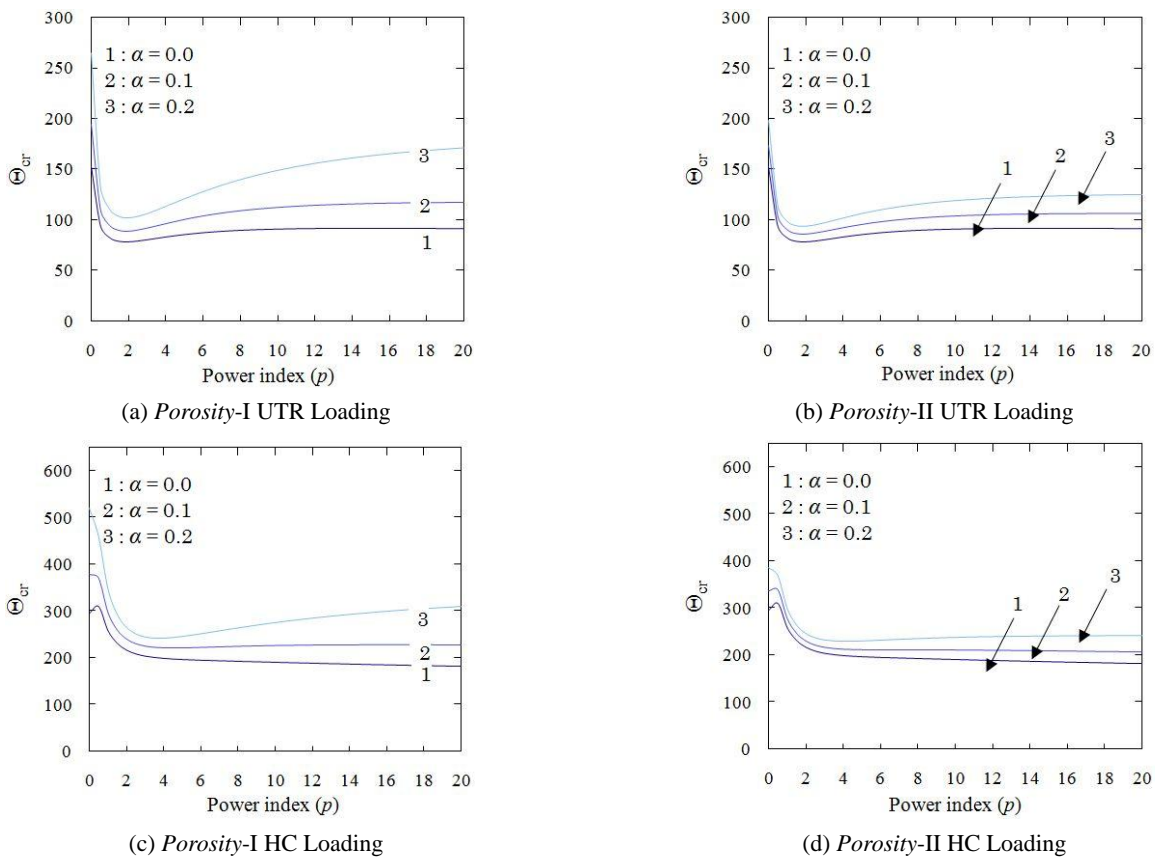


Fig. 2 Variations of the critical buckling temperature of a porous annular nanoplate under different types of thermal loading and porosity distribution with respect to power index for various values of porosity volume fraction ($\mu = 2(\text{nm})^2, \beta = 0.3, \delta = 0.015, k_w = 100, k_g = 10$)

Winkler and Pasternak coefficients, the thermal buckling load and number of nodal diameters of the nanoplate increase which is expected since the elastic stiffness of the nanostructure enhances. In addition, it is observed that by increasing the elastic foundation parameters of annular FG nanoplates, buckling temperature difference will increase too and this behavior is more significant for FG nanoplates

under HC thermal loading. Interesting results are observed for the case of higher modes of buckling configuration. As seen in Table 5, the effect of nonlocal parameter on critical buckling temperatures increases for annular nanoplates under higher modes of buckling configuration. It is again verified that increasing of nonlocal parameter leads to lower critical buckling temperature difference, especially for

annular nanoplates with higher modes of buckled shape.

Fig. 2 demonstrates the effects of porosity distributions and thermal loading on the buckling temperature difference of FG nanoplates under various values of porosity volume fraction versus power index. It is obvious that as the porosity parameter increases, the critical buckling temperature rise increases, independently of the types of thermal loading. Therefore, a porous annular nanoplate has larger critical buckling temperatures than a perfect one. Another interesting observation is that there is a large gap as increasing of the power exponent. In fact, with the increase of power law index, the influence of porosity increases. The buckling temperature also decreases for increasing values of the power index from 0 up to 2. This is due to the fact that for large values of power law index, the material properties of the nanoplate become similar to the material properties of a metal with higher thermal expansion coefficients in comparison to the ceramic. Thus, one could easily control the critical buckling temperature of the porous annular nanoplate by tuning the power index and porosity volume fraction.

The variation of the critical buckling temperature rise with respect to the δ ratio under UTR loading and uneven distribution for various values of elastic substrate and nonlocal parameters is computed and shown in Fig. 3. This

figure indicates that for a given value of nonlocal parameter, increasing the δ ratio, the buckling temperature increases. Also, it can be seen that the nonlocal parameter decreases the buckling temperature since the nonlocal parameter decreases the stiffness of annular nanoplates. Since the radius of the nanoplate is kept constant, the bending stiffness of the annular plate increases due to an increase in thickness, which consequently results in increment of the critical temperature. Also, the elastic substrate has an increasing effect on buckling temperatures of porous nanoplates. In fact, increasing in Winkler and Pasternak coefficients supplies enhancement of stiffness of annular nanoplate.

The variation of the critical temperature with β ratio is investigated in Fig. 4, where it is visible that an annular nanoplate with a large β ratio undergoes a large critical temperature difference. In this figure, both even and uneven porosity distributions are considered. It is noted that each circle in this figure indicates an increase in the number of nodal diameters of the buckled mode. This figure also demonstrates that the number of nodal diameters changes, when the inner to outer radius ratio, β increases from 0.1 to 0.8.

In Fig. 5, the critical buckling temperature is depicted with respect to two cases of thermal loading and various

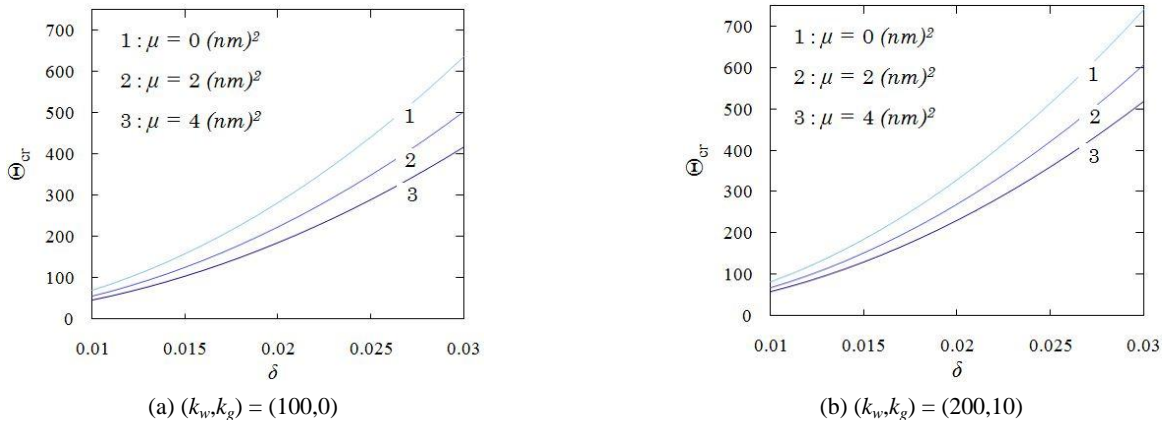


Fig. 3 Variations of critical buckling temperature of the Porosity-II annular nanoplate under UTR loading with respect to δ ratio for various values of elastic substrate and nonlocal parameters ($\alpha = 0.2, p = 1, \beta = 0.5$)

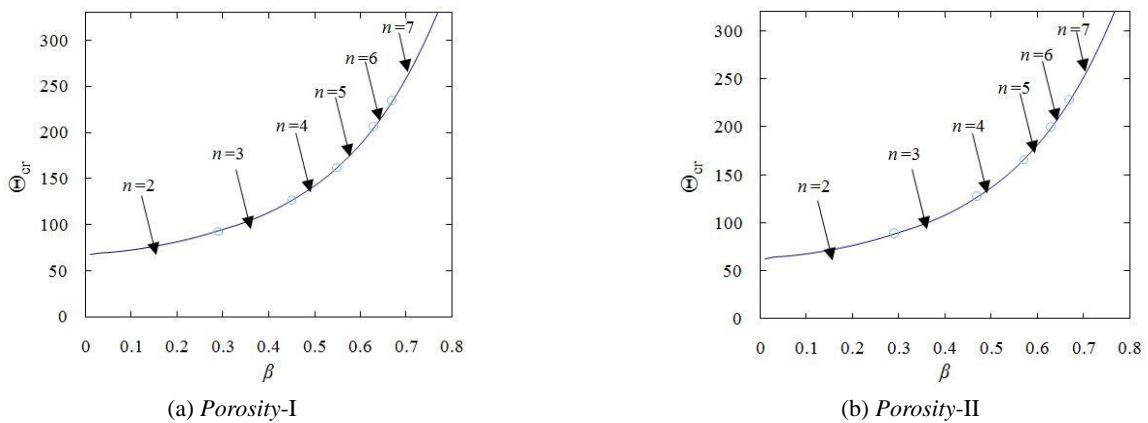


Fig. 4 Variations of the critical buckling temperature of a porous annular nanoplate under UTR loading with respect to β ratio for two types of porosity distribution ($p = 1, \mu = 2 \text{ (nm)}^2, \alpha = 0.1, \delta = 0.015, k_w = 100, k_g = 10$)

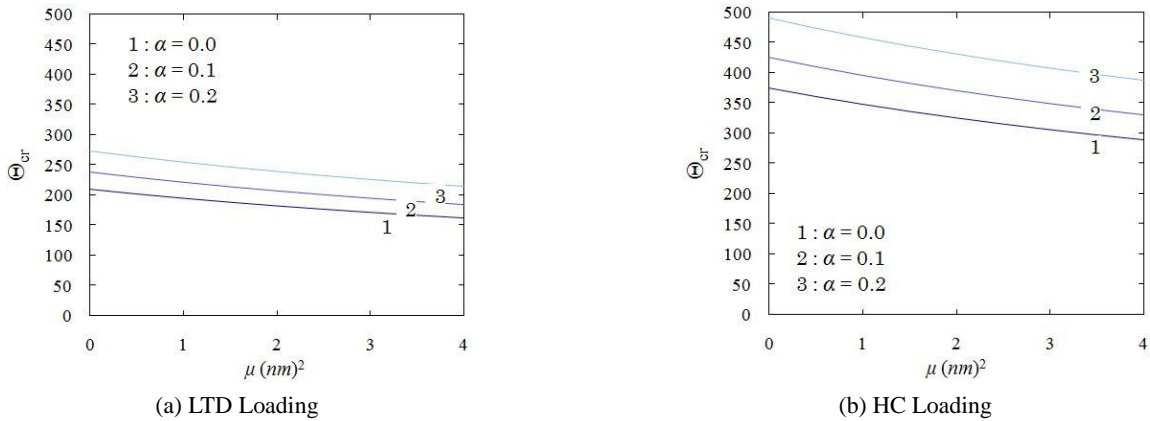


Fig. 5 Variations of critical buckling temperature of the Porosity-I annular nanoplate under different types of thermal loading with respect to nonlocal parameter for various values of porosity volume fraction ($p = 1$, $\beta = 0.4$, $\delta = 0.015$, $k_w = 200$, $k_g = 10$)

values of porosity volume fraction for varying nonlocal parameters. It can be seen that porosities inside the nanomaterial lead to higher critical buckling temperature by increase the stiffness of annular nanoplate. Again, an annular nanoplate with porosities has larger buckling temperature than a perfect one. The buckling temperature also decreases for increasing values of the nonlocal parameter from 0 up to 4 $(nm)^2$. The reason of this phenomenon is due to the reduced bending stiffness of the annular nanoplate with porosities. Also, it is found that the discrepancy between critical buckling temperature difference of perfect annular FG plates ($\alpha = 0$) and that of nanoplate with porosities is more significant in HC thermal loading in comparison with other types of thermal loading.

8. Conclusions

In this paper, asymmetric thermal buckling characteristic of annular nanoplates under two types of porosity distribution has been proposed based on the nonlocal elasticity theory. A modified power law function has been employed to describe the graded material properties. With the aid of a von-Kármán type of geometrical nonlinearity and static version of Hamilton's principle, the complete set of equilibrium equations considering the asymmetric deformations of the nanoplate is obtained. Pre-buckling analysis is presented to find the distribution of stresses and deformations prior to thermal buckling. Afterwards, based on the adjacent equilibrium criterion, nonlocal stability equations are established. These equations have been solved via exact analytical solutions to obtain critical buckling temperatures.

Thus, we examined the effect of the material gradation, different types of thermal loading and porosity distribution, elastic coefficients, porosity and nonlocal parameters and geometrical dimensions, on the thermal buckling characteristics. Based on this parametric research, it is found that these parameters have a significant effect on the thermal buckling behavior of porous nanostructures. The effects can be summarized as follows

- It was seen that the critical buckling temperature of nanoplate from maximum to minimum may be sorted, in order, HC, LTD, and UTR, and this prediction is the same for all values of nonlocal parameter and elastic foundation coefficients. Also, thermal buckling does not exist generally for annular nanoplates with porosities unless boundary conditions are of clamped type.
- The critical temperature difference increases as the porosity volume fraction increases, whereas the buckling temperature decreases when the applied porosity distribution changes from even to uneven.
- It was observed that by increasing the elastic foundation parameters of annular FG nanoplates, buckling temperature difference and number of nodal diameters will increase too and this behavior is more significant for nanoplates under HC thermal loading and higher modes of buckling configuration.
- It was indicated that increasing of nonlocal parameter leads to lower buckling temperature difference, especially for porous annular nanoplates with higher modes of buckled shape and β ratio.
- For all cases of thermal loading, the effect of nonlocal parameter on critical buckling temperatures increases for annular nanoplates under higher modes of buckling configuration. In other words, by increasing the influence of small scale effect, the stiffness of annular FG nanoplates decreases.
- The buckling temperature of nanoplate decreases with an increasing power index because of the material degradation due to the enrichment of the metal constituent.
- It was shown that the discrepancy between critical buckling temperature difference of perfect annular plates and that of FG nanoplate with porosities is more significant in HC thermal loading in comparison with other types of thermal loading.

References

- Akgoz, B. and Civalek, O. (2011a), "Nonlinear vibration analysis of laminated plates resting on nonlinear two-parameters elastic foundations", *Steel Compos. Struct., Int. J.*, **11**(5), 403-421.
- Akgöz, B. and Civalek, Ö. (2011b), "Buckling analysis of cantilever carbon nanotubes using the strain gradient elasticity and modified couple stress theories", *J. Computat. Theor. Nanosci.*, **8**(9), 1821-1827.
- Akgöz, B. and Civalek, Ö. (2016), "Static and dynamic response of sector-shaped graphene sheets", *Mech. Adv. Mater. Struct.*, **23**(4), 432-442.
- Ashoori, A. and Vanini, S.S. (2016a), "Thermal buckling of annular microstructure-dependent functionally graded material plates resting on an elastic medium", *Compos. Part B: Eng.*, **87**, 245-255.
- Ashoori, A. and Vanini, S.S. (2016b), "Nonlinear thermal stability and snap-through behavior of circular microstructure-dependent FGM plates", *Eur. J. Mech.-A/Solids*, **59**, 323-332.
- Ashoori, A. and Vanini, S.S. (2017a), "Nonlinear bending, postbuckling and snap-through of circular size-dependent functionally graded piezoelectric plates", *Thin-Wall. Struct.*, **111**, 19-28.
- Ashoori, A. and Vanini, S.S. (2017b), "Vibration of circular functionally graded piezoelectric plates in pre-/postbuckled configurations of bifurcation/limit load buckling", *Acta Mechanica*, **228**(9), 2945-2964.
- Ashoori, A., Salari, E. and Vanini, S.S. (2016), "Size-dependent thermal stability analysis of embedded functionally graded annular nanoplates based on the nonlocal elasticity theory", *Int. J. Mech. Sci.*, **119**, 396-411.
- Ashoori, A., Vanini, S.S. and Salari, E. (2017), "Size-dependent axisymmetric vibration of functionally graded circular plates in bifurcation/limit point instability", *Appl. Phys. A*, **123**(4), 226.
- Avcar, M. (2016), "Effects of material non-homogeneity and two parameter elastic foundation on fundamental frequency parameters of timoshenko beams", *Acta Physica Polonica A*, **130**(1), 375-378.
- Aydogdu, M., Arda, M. and Filiz, S. (2018), "Vibration of axially functionally graded nano rods and beams with a variable nonlocal parameter", *Adv. Nano Res., Int. J.*, **6**(3), 257-278.
- Bagheri, H., Kiani, Y. and Eslami, M. (2017), "Asymmetric thermal buckling of annular plates on a partial elastic foundation", *J. Thermal Stresses*, **40**(8), 1015-1029.
- Bagheri, H., Kiani, Y. and Eslami, M. (2018), "Asymmetric thermal buckling of temperature dependent annular FGM plates on a partial elastic foundation", *Comput. Math. Applicat.*, **75**(5), 1566-1581.
- Baltacıoğlu, A.K., Akgöz, B. and Civalek, Ö. (2010), "Nonlinear static response of laminated composite plates by discrete singular convolution method", *Compos. Struct.*, **93**(1), 153-161.
- Baltacıoğlu, A., Civalek, Ö., Akgöz, B. and Demir, F. (2011), "Large deflection analysis of laminated composite plates resting on nonlinear elastic foundations by the method of discrete singular convolution", *Int. J. Press. Vessels Piping*, **88**(8-9), 290-300.
- Bedroud, M., Nazemnezhad, R. and Hosseini-Hashemi, S. (2015), "Axisymmetric/asymmetric buckling of functionally graded circular/annular Mindlin nanoplates via nonlocal elasticity", *Meccanica*, **50**(7), 1791-1806.
- Bouadi, A., Bousahla, A.A., Houari, M.S.A., Heireche, H. and Tounsi, A. (2018), "A new nonlocal HSDT for analysis of stability of single layer graphene sheet", *Adv. Nano Res., Int. J.*, **6**(2), 147-162.
- Brush, D.O. and Almroth, B.O. (1975), *Buckling of Bars, Plates, and Shells*, New York, McGraw-Hill Book Co.
- Chen, W.J. and Li, X.P. (2013), "Size-dependent free vibration analysis of composite laminated Timoshenko beam based on new modified couple stress theory", *Arch. Appl. Mech.*, **83**(3), 431-444.
- Civalek, Ö. (2006), "The determination of frequencies of laminated conical shells via the discrete singular convolution method", *J. Mech. Mater. Struct.*, **1**(1), 163-182.
- Civalek, Ö. (2008), "Analysis of thick rectangular plates with symmetric cross-ply laminates based on first-order shear deformation theory", *J. Compos. Mater.*, **42**(26), 2853-2867.
- Civalek, Ö. (2013), "Nonlinear dynamic response of laminated plates resting on nonlinear elastic foundations by the discrete singular convolution-differential quadrature coupled approaches", *Compos. Part B: Eng.*, **50**, 171-179.
- Civalek, Ö. (2017), "Free vibration of carbon nanotubes reinforced (CNTR) and functionally graded shells and plates based on FSDT via discrete singular convolution method", *Compos. Part B: Eng.*, **111**, 45-59.
- Civalek, Ö. and Demir, C. (2011), "Buckling and bending analyses of cantilever carbon nanotubes using the euler-bernoulli beam theory based on non-local continuum model", *Asian J. Civil Eng.*, **12**(5), 651-661.
- Dastjerdi, S. and Akgöz, B. (2018), "New static and dynamic analyses of macro and nano FGM plates using exact three-dimensional elasticity in thermal environment", *Compos. Struct.*, **192**, 626-641.
- Demir, Ç., Mercan, K. and Civalek, Ö. (2016), "Determination of critical buckling loads of isotropic, FGM and laminated truncated conical panel", *Compos. Part B: Eng.*, **94**, 1-10.
- Ebrahimi, F. and Salari, E. (2015a), "Thermal buckling and free vibration analysis of size dependent Timoshenko FG nanobeams in thermal environments", *Compos. Struct.*, **128**, 363-380.
- Ebrahimi, F. and Salari, E. (2015b), "Thermo-mechanical vibration analysis of nonlocal temperature-dependent FG nanobeams with various boundary conditions", *Compos. Part B: Eng.*, **78**, 272-290.
- Ebrahimi, F. and Salari, E. (2016a), "Effect of various thermal loadings on buckling and vibrational characteristics of nonlocal temperature-dependent functionally graded nanobeams", *Mech. Adv. Mater. Struct.*, **23**(12), 1379-1397.
- Ebrahimi, F. and Salari, E. (2016b), "Thermal loading effects on electro-mechanical vibration behavior of piezoelectrically actuated inhomogeneous size-dependent Timoshenko nanobeams", *Adv. Nano Res., Int. J.*, **4**(3), 197-228.
- Ebrahimi, F., Ghasemi, F. and Salari, E. (2016), "Investigating thermal effects on vibration behavior of temperature-dependent compositionally graded Euler beams with porosities", *Meccanica*, **51**(1), 223-249.
- Ehyaeei, J., Ebrahimi, F. and Salari, E. (2016), "Nonlocal vibration analysis of FG nano beams with different boundary conditions", *Adv. Nano Res., Int. J.*, **4**(2), 85-111.
- Eringen, A.C. (1983), "On differential equations of nonlocal elasticity and solutions of screw dislocation and surface waves", *J. Appl. Phys.*, **54**(9), 4703-4710.
- Fang, X.-Q. and Zhu, C.-S. (2017), "Size-dependent nonlinear vibration of nonhomogeneous shell embedded with a piezoelectric layer based on surface/interface theory", *Compos. Struct.*, **160**, 1191-1197.
- Fang, X.-Q., Zhu, C.-S., Liu, J.-X. and Liu, X.-L. (2018a), "Surface energy effect on free vibration of nano-sized piezoelectric double-shell structures", *Physica B: Condensed Matter*, **529**, 41-56.
- Fang, X.-Q., Zhu, C.-S., Liu, J.-X. and Zhao, J. (2018b), "Surface energy effect on nonlinear buckling and postbuckling behavior of functionally graded piezoelectric cylindrical nanoshells under lateral pressure", *Mater. Res. Express*, **5**(4), 045017.
- Gürses, M., Civalek, Ö., Korkmaz, A.K. and Ersoy, H. (2009), "Free vibration analysis of symmetric laminated skew plates by

- discrete singular convolution technique based on first-order shear deformation theory”, *Int. J. Numer. Methods Eng.*, **79**(3), 290-313.
- Kiani, Y. and Eslami, M. (2013), “An exact solution for thermal buckling of annular FGM plates on an elastic medium”, *Compos. Part B: Eng.*, **45**(1), 101-110.
- Li, L. and Hu, Y. (2017), “Post-buckling analysis of functionally graded nanobeams incorporating nonlocal stress and microstructure-dependent strain gradient effects”, *Int. J. Mech. Sci.*, **120**, 159-170.
- Lü, C., Lim, C.W. and Chen, W. (2009), “Size-dependent elastic behavior of FGM ultra-thin films based on generalized refined theory”, *Int. J. Solids Struct.*, **46**(5), 1176-1185.
- Mechab, B., Mechab, I., Benaissa, S., Ameri, M. and Serier, B. (2016), “Probabilistic analysis of effect of the porosities in functionally graded material nanoplate resting on Winkler–Pasternak elastic foundations”, *Appl. Math. Model.*, **40**(2), 738-749.
- Mercan, K. and Civalek, Ö. (2016), “DSC method for buckling analysis of boron nitride nanotube (BNNT) surrounded by an elastic matrix”, *Compos. Struct.*, **143**, 300-309.
- Mercan, K. and Civalek, Ö. (2017), “Buckling analysis of Silicon carbide nanotubes (SiCNTs) with surface effect and nonlocal elasticity using the method of HDQ”, *Compos. Part B: Eng.*, **114**, 34-45.
- Reddy, J. (2007), “Nonlocal theories for bending, buckling and vibration of beams”, *Int. J. Eng. Sci.*, **45**(2-8), 288-307.
- Shahba, A., Attarnejad, R. and Hajilar, S. (2011), “Free vibration and stability of axially functionally graded tapered Euler-Bernoulli beams”, *Shock Vib.*, **18**(5), 683-696.
- She, G.-L., Ren, Y.-R., Yuan, F.-G. and Xiao, W.-S. (2018), “On vibrations of porous nanotubes”, *Int. J. Eng. Sci.*, **125**, 23-35.
- Shen, J., Wang, H. and Zheng, S. (2018), “Size-dependent pull-in analysis of a composite laminated micro-beam actuated by electrostatic and piezoelectric forces: Generalized differential quadrature method”, *Int. J. Mech. Sci.*, **135**, 353-361.
- Shojaeefard, M.H., Googarchin, H.S., Ghadiri, M. and Mahinzare, M. (2017), “Micro temperature-dependent FG porous plate: free vibration and thermal buckling analysis using modified couple stress theory with CPT and FSDT”, *Appl. Math. Model.*, **50**, 633-655.
- Wang, Q. (2005), “Wave propagation in carbon nanotubes via nonlocal continuum mechanics”, *J. Appl. Phys.*, **98**(12), 124301.
- Wang, C. and Wang, C.Y. (2004), *Exact Solutions for Buckling of Structural Members*, CRC press.
- Wang, Q., Shi, D., Liang, Q. and Shi, X. (2016), “A unified solution for vibration analysis of functionally graded circular, annular and sector plates with general boundary conditions”, *Compos. Part B: Eng.*, **88**, 264-294.
- Wattanasakulpong, N. and Ungbhakorn, V. (2014), “Linear and nonlinear vibration analysis of elastically restrained ends FGM beams with porosities”, *Aerosp. Sci. Technol.*, **32**(1), 111-120.
- Wattanasakulpong, N. and Chaikittiratana, A. (2015), “Flexural vibration of imperfect functionally graded beams based on Timoshenko beam theory: Chebyshev collocation method”, *Meccanica*, **50**(5), 1331-1342.
- Zhang, X., Qian, Y., Zhu, Y. and Tang, K. (2014), “Synthesis of Mn₂O₃ nanomaterials with controllable porosity and thickness for enhanced lithium-ion batteries performance”, *Nanoscale*, **6**(3), 1725-1731.
- Zhu, C.-S., Fang, X.-Q., Liu, J.-X. and Li, H.-Y. (2017), “Surface energy effect on nonlinear free vibration behavior of orthotropic piezoelectric cylindrical nano-shells”, *Eur. J. Mech.-A/Solids*, **66**, 423-432.